J Mar Sci Technol (2011) 16:311–322
DOI 10.1007/s00773-011-0128-z

ORIGINAL ARTICLE

A new weather-routing system that accounts for ship stability based on a real-coded genetic algorithm

Atsuo Maki · Youhei Akimoto · Yuichi Nagata · Shigenobu Kobayashi · Eiichi Kobayashi · Shigeaki Shiotani · Teruo Ohsawa · Naoya Umeda

Received: 28 September 2010 / Accepted: 16 April 2011 / Published online: 2 August 2011

Abstract The operation schedule of an oceangoing vessel can be influenced by wave or wind disturbances, and is therefore weather routed. The weather-routing problem is considered to be a multimodal function problem. Therefore, in the present research, the real-coded genetic algorithm technique (an evolutionary calculation technique) is applied to globally search for the optimum route. Additionally, to avoid maritime accidents due to parametric rolling, this route optimization method takes into account the risk of parametric rolling as one of its objective functions. Numerical verification is carried out for three kinds of objective functions with different weight ratios between fuel efficiency and ship safety in parametric rolling. As a result, it is numerically confirmed that the relation between economics and ship safety is a trade-off, and the safer route is not necessarily the most economical. Considering its robustness, the proposed method appears to be a powerful practical tool by choosing the most appropriate weights for economics and ship safety.

Keywords Weather-routing · Ship stability · Real-coded genetic algorithm

A. Maki · E. Kobayashi (✉) · S. Shiotani · T. Ohsawa
Graduate School of Maritime Sciences, Kobe University,
5-1-1 Fukae-Minami, Higashinada, Kobe 658-0022, Japan
e-mail: kobayasi@harbor.kobe-u.ac.jp

Present Address:
A. Maki
Naval Systems Research Center, Technical Research & Development Institute, Ministry of Defense, 2-2-1 Nakameguro, Meguro, Tokyo 153-8630, Japan

Y. Akimoto · Y. Nagata · S. Kobayashi
Interdisciplinary Graduate School of Science and Engineering, Tokyo Institute of Technology, 4259 Natatsuta, Midoriku, Yokohama 226-8502, Japan

N. Umeda
Department of Naval Architecture and Ocean Engineering, Graduate School of Engineering, Osaka University,
2-1 Yamadaoka, Suita, Osaka 565-0971, Japan

1 Introduction

The route optimization technique for oceangoing vessels—known as weather routing—is widely applied, and a considerable number of studies of it have been carried out [1, 2]. Existing methods, however, have primarily formulated the problem of minimum time or minimum fuel consumption with constraints, and so a method that accounts for ship stability has not generally been proposed. As mentioned below, when a ship travels in an ocean, phenomena such as parametric rolling, which lead to dangerous situations for the ship or its cargo, can be triggered [3]. Therefore, the present research proposes a route optimization method that considers not only fuel efficiency but also individual ship stability.

Serious accidents involving parametric rolling of modern container ships and pure car/truck carriers (PCTCs) have been reported in recent years [3]. In late October 1998, a post-Panamax C11 class container ship eastbound from Kaohsiung to Seattle was overtaken by a violent storm in the North Pacific Ocean and sustained extensive loss of and serious damage to deck-stowed containers due to parametric rolling; the maximum roll angle was reported to be as great as 35°–40° [4]. The vessel was weather routed on her transpacific voyage, and also received regular reports and forecasts from the Japanese Meteorological Office and the US National Weather Service [4]. In general, existing weather-routing methods are constructed to

generate the optimum route to minimize fuel consumption from an economical point of view, and ship safety is taken into account as an operational limit [2]. However, to avoid marine accidents due to dangerous phenomena such as parametric rolling, the danger should be considered at the stage of course selection.

Typically, weather routing is modeled as a minimum time problem or a minimum fuel consumption problem subject to some constraints, and the obtained problem is solved with an optimization method. Basically, optimization methods can be categorized into two types: the single-point search method and the multipoint search method. It is well known that the multipoint search method is more suitable for optimizing a multimodal function problem, such as the weather-routing problem, than the single-point search method. Additionally, in general, genetic algorithms (GAs)—which are multipoint search methods—perform more robustly than gradient-based approaches on highly multimodal objective functions. Furthermore, GAs show more robustness in terms of the selection of the initial value. Therefore, in this paper a real-coded genetic algorithm (RCGA) [5, 6] was applied.

Using the proposed method, we succeeded in (1) obtaining the optimal route with strong robustness, and (2) accounting for the danger of parametric rolling during course optimization. Then, by carrying out numerical experiments, we confirmed the effectiveness of the proposed method.

2 Summary of the present method

The weather-forecasting data used here consist of the wind and waves predicted by National Center for Environmental Prediction (NCEP). The data are renewed at intervals of 6 h, and the data at each prediction time until 180 h are included. These data consist of wind speed, wind direction, significant wave height, mean wave period and wave direction. Concerning the wave data, the data denoted "primary wave" are utilized for this paper's calculations. Although two components, wind wave and swell, are included in these data, the wave spectrum is assumed to be the International Towing Tank Conference (ITTC) spectrum, and the wave-directional concentration parameter is a cos-2 function for short-term predictions. However, to calculate the parametric rolling probability in this paper, the wave spectrum is assumed to be a modified PM-type spectrum, and the wave-directional concentration parameter is a cos-infinity function. The reason why the assumed spectra for the two estimations are different is that weather forecasting data with wave and swell components cannot be obtained separately. Although improved data will be required for future tasks, the data used here is considered to be sufficient to verify the present method. In addition, data provided by the National Oceanic and Atmospheric Administration (NOAA), which covers an average of 5 days, is also used. The data used for wind and wave forecasts from the NOAA/NCEP operational global forecasting system (GFS) (http://www.nco.ncep.noaa.gov/pmb/products/gfs/) and wave model (WAVEWATCH III), and the comprehensive error statistics are presented on the WAVEWATCH III model home page (http://polar.ncep.noaa.gov/waves/). According to the model validations (http://polar.ncep.noaa.gov/waves/validation.shtml), the wind has a root-mean-square-error (RMSE) of around 2 m/s for the 24 h forecast and 3–4.5 m/s for the 120 h forecast. As for the significant wave height, the RMSE is 0.3–0.7 m for the 24 h forecast and 0.6–1.4 m for the 120 h forecast.

Although route optimization calculations should be carried out every day during a voyage, as a first step in this research, optimization is carried out only for the first day of the voyage, before departure. Furthermore, we assume that the forecasted weather actually occurs.

In the proposed method, the latitudes of the waypoints and the propeller revolution numbers are treated as control variables, as described in the following section, and it is assumed that the ship's course does not deviate from the determined course between two waypoints. The ship's route is determined as the straight line joining two waypoints as control variables on the Mercator chart, and the distance or course between them is calculated by Mercator sailing. Also, only the surge speed variation due to waves, wind and current is considered; other motion modes are ignored for the sake of brevity. Therefore, except for its treatment of the objective function and other minor differences, the present method is considered to be an extension of the method proposed by Tsujimoto and Tanizawa [2]. Finally, the initial route for route optimization is set to be the great-circle route joining the departure and arrival points.

To estimate the surge speed in irregular seas, a short-term prediction of the added resistance is obtained by using the Research Initiative on Oceangoing Ships (RIOS) system developed at Osaka University. In this method, the added resistance is estimated with Maruo's theory [7], and the Kochin function is estimated by Kashiwagi's slender body theory, known as the enhanced unified theory (EUT) [8, 9]. The wind force in the surge direction acting on the hull is estimated by Fujiwara's method [10].

3 Safety assessment of the ship

A feature of this research is that the risk of parametric rolling is taken into account in the route optimization. In the present research, the probability for unit time is applied as the risk of parametric rolling. This probability is

estimated using the method proposed by Maki et al. [11], and an explanation of parametric rolling and the method for estimating its probability is briefly summarized in the following.

Parametric rolling is induced by a time-varying restoring arm [3]. In general, this phenomenon occurs in a ship with a hull form that produces a large change in the restoring arm in waves, such as those of modern container ships or PCTCs [3] due to their exaggerated bow flares and transom sterns. Once parametric rolling occurs, the maximum roll angle can reach 40° or more. Hence, serious accidents caused by this phenomenon have been reported in recent years. Nevertheless, few methods of predicting the parametric rolling probability have been presented since Blocki's research [12]. In the present research, the method proposed by Maki et al. [11] is utilized. Here, ship response in regular seas is estimated by solving the averaged system of the original 1-DOF roll model, and the random waves necessary for the occurrence of parametric rolling are applied based on wave group theory [13]. In this method, the initial heel angle is required to numerically simulate the averaged 1-DOF roll system, so a parametric rolling probability with an initial heel angle of 2° is utilized. The initial roll amplitude must be set, as an initial value of zero amplitude gives a trajectory with zero amplitude. A detailed explanation of this can be found in the literature [11].

Following the work of Tsujimoto and Tanizawa [2], the service limitation of the short-term predictive value of the acceleration at the bow section is set to be 80% of the gravitational acceleration. Here, the value is estimated by RIOS. This service limitation is included in the constraints of the route optimization problem so that a ship route through a sea area in which the pitch motion exceeds this limitation is not be generated.

4 Real-coded genetic algorithm

The weather-routing problem can be formulated as an optimization problem in a continuous domain,

$$\min_x f(x),\ x \in S \subseteq \mathbf{R}^n, \tag{1}$$

where $f(x)$ is the objective function to be minimized and S is the feasible set, which is often an intersection of sets $\{x|g_i(x) \leq 0\}$. The traditional approach to minimization is based on the gradient method, which exploits the differentiability, twice differentiability or convexity of the objective function $f(x)$ and constraint function $g_i(x)$. In contrast, evolutionary approaches (e.g., GAs) only need to know whether the search point is feasible, and—if the point is feasible—the values of the objective function. Therefore, evolutionary approaches are suitable for black-box scenarios of the weather-routing problem that require a computer simulation to evaluate objective functions and that satisfy neither the differentiability nor the convexity requirements.

For optimization in a continuous domain, two types of GAs can be used: one is the bit-string GA, in which a binary string (a sequence of zeros and ones) is considered as a genotype, and the other is the real-coded GA (see [5, 6]), in which real-valued vectors are considered as genotypes. For problems in which there are strong intervariable dependencies, the computational efficiency of the bit-string GA becomes extremely poor. This is because the real number vector must be represented by a binary string, and a crossover operator that ignores the intervariable dependency is used within the framework of the bit-string GA. Therefore, it is often reported that the population does not converge but stagnate. In such a case, a highly accurate solution cannot be obtained. In general, the encoding used in the real-coded GA is more natural for continuous search spaces and leads to better performance [6]. Therefore, for the weather-routing problem, which includes intervariable dependency, real-coded GA is expected to be the best option. Real-coded GAs consist of a crossover operator, which produces new candidate solutions, and a selection model, which determines the next population (the set of feasible solutions).

In real-coded GAs, the crossover is the main operator for producing new candidate solutions. BLX-α [5] was the first successful algorithm that did not require a mutation operator. The limitation of BLX-α is that the search fails on variable-dependent functions. To solve this problem, UNDX [6] was proposed. Based on the success of UNDX, Kita et al. [14] theoretically analyzed the UNDX operator. Using these results, Kita and Yamamura [15] proposed design guides for real-coded GAs. The guideline for sampling new points suggests that a crossover is needed to generate offspring points over the analogous region covered by the parental points. More precisely, it states that the statistics of parents, such as the mean vector and covariance matrix, should be preserved over the crossover operation. Based on the preservation of statistics, crossovers using more than two parents, such as UNDX-m [16], SPX [17], and LUNDX-m [18], have been proposed. Kobayashi [19] has compared these crossovers with respect to the shape of the crossover distribution and proposed the real-coded ensemble crossover REX$^{\text{star}}$ as the generalization of UNDX-m.

The just generation gap (JGG) selection model was proposed by Akimoto et al. [20, 21] as a selection model for multi-parental crossovers, and it showed that GAs which combine a multi-parental crossover with the JGG selection model outperform those which include the minimal generation gap (MGG) model [22], which is a standard selection model for two parental crossovers. In this paper,

as it is one of the current best choices, we use the real-coded GA that combines REX^{star} with the JGG selection model to solve the weather-routing problem.

5 Objective functions

In this section, we discuss the control variables, objective functions and constraint functions. The vector of the control variables consists of the latitude of the waypoints and the propeller revolution numbers in the segments between two waypoints. Therefore, the latitude of the waypoints is optimized, although their longitudes are fixed. Further, the propeller revolution number is assumed to be constant in each segment. The control vector x can then be represented as

$$x \equiv (Lat_1, \ldots, Lat_{INode}, PN_1, \ldots, PN_{INode+1})^T, \tag{2}$$

where Lat_i represents the latitude of ith waypoint, PN_i is the propeller revolution number in ith segment, and INode is the number of waypoints. The performance indices and constraints are a function of x, as follows:

Objective function f_1: the ratio of the energies required for voyage A and voyage B; that is, $f_1 \equiv E_B/E_A$. Here, E_A is the energy for voyage A, in which the ship is directed along the great-circle course with a constant propeller revolution number. The procedure to find the value of the constant propeller revolution number is stated in Sect. 8. In contrast, E_B is the energy for voyage B, in which the ship is directed along the generated route with the propeller revolution number generated by the optimization method. The values E_A and E_B are calculated by the propeller revolution number and the effective horsepower in the time domain.

Objective function f_2: the maximum parametric rolling probability during the voyage.

Constraint g_1: the inequality constraint of the time of arrival. Here, the imposed time difference between the expected time of arrival (ETA) and the actual time of arrival (ATA) is <30 min, and delayed arrival is prohibited. Therefore, these conditions can be represented as the following inequality constraint:

$$(\mathrm{ETA} - \mathrm{ATA})(\mathrm{ETA} - \mathrm{ATA} - 1800) \leq 0. \tag{3}$$

The measurement units of this equation are seconds.

Constraint $g_{2,i}(1 \leq i \leq \mathrm{INode} + 1)$: the inequality constraint of the acceleration at bow section a_F in each segment. Here, $a_F \leq 0.8g$ is imposed, where g represents the gravitational acceleration.

Constraint $g_{3,i}(1 \leq i \leq \mathrm{INode})$: the inequality constraint of the latitude of each nodal point; i.e., the waypoint, Lat_i. Here, $0.01 \leq \mathrm{Lat}_i \leq 59.99$ is imposed.

Constraint $g_{4,i}(1 \leq i \leq \mathrm{INode} + 1)$: the inequality constraint of the propeller revolution number PN_i in each segment. Here, $1.0 \leq PN_i \leq 4.0$ is imposed.

In the above, f_1, f_2, g_1 and $g_{2,i}$ cannot be evaluated until the numerical simulation, whereas $g_{3,i}$ and $g_{4,i}$ can be evaluated without the simulation. Therefore, since the objective functions and constraints are different, the optimization problem in the present research is defined as Eqs. 4–6 using the penalty function method, as follows:

$$\text{minimize:} \quad F = h_1(f_1(x)) + h_2(\log_{10}(f_2(x))) + h_3(\max(g_1(x), 0)) + h_4\left(\sum_{i=1}^{\mathrm{INode}+1} \max\left(g_{2,i}(x), 0\right)\right) \tag{4}$$

$$\text{subject to:} \quad 0.01 \leq x_i \leq 59.99 \quad \text{for } i = 1, 2, \ldots, \mathrm{INode}, \tag{5}$$

$$1 \leq x_i \leq 4 \quad \text{for } i = \mathrm{INode} + 1, 2, \ldots, 2\,\mathrm{INode} + 1. \tag{6}$$

In Eq. 4, h_1, h_2, h_3 and h_4 represent monotonically increasing functions that adjust the scale. Here h_1, h_3 and h_4 are set to be identity functions and h_2 is a common logarithmic function. It should be noted that the allowable failure probability of the structure is generally considered to be 10^{-6} to 10^{-7} per year [23]. Therefore, in the present research, we assume that the risk of parametric rolling can be ignored if the parametric rolling probability is $<10^{-6}$ per year. However, the result obtained using Maki's et al. method is expressed as the probability for unit time, so that the threshold value 10^{-6} is translated to the occurrence probability for unit time; that is, 3.17×10^{-14}. A detailed explanation of this is shown in the "Appendix." Based on this consideration, the following three objective functions are applied in the present research:

In the case of a weight ratio of 10:1 between $f_1(x)$ and $\log_{10}(f_2(x))$:

$$\mathrm{Obj1}(x) = 10f_1(x) + \max(\log_{10}(f_2(x)) - \log_{10}\left(3.17 \times 10^{-14}\right), 0) + \max(g_1(x), 0) + \sum_{i=1}^{\mathrm{INode}+1} \max\left(g_{2,i}(x), 0\right). \tag{7}$$

In the case of a weight ratio of 10:0 between $f_1(x)$ and $\log_{10}(f_2(x))$:

$$\mathrm{Obj2}(x) = 10f_1(x) + \max(g_1(x), 0) + \sum_{i=1}^{\mathrm{INode}+1} \max\left(g_{2,i}(x), 0\right). \tag{8}$$

In the case of a weight ratio of 10:0.1 between $f_1(x)$ and $\log_{10}(f_2(x))$:

$$\mathrm{Obj3}(x) = 10f_1(x) + 0.1\max(\log_{10}(f_2(x)) - \log_{10}\left(3.17 \times 10^{-14}\right), 0) + \max(g_1(x), 0) + \sum_{i=1}^{\mathrm{INode}+1} \max\left(g_{2,i}(x), 0\right). \tag{9}$$

Obj1, Obj2 and Obj3 are different from each other due to the weights of $f_1(x)$ and $\log_{10}(f_2(x))$. Here, considering the order relation between $f_1(x)$ and $\log_{10}(f_2(x))$, we can roughly estimate their orders as $f_1(x) \approx O(1)$ and $\log_{10} f_2(x) \approx O(10)$. Therefore, the weight value of $f_1(x)$ is chosen to be larger than that of $\log_{10}(f_2(x))$. Further, note that the contribution of $f_2(x)$ to the objective function disappears in Obj2. When this objective function is utilized, only the optimization of fuel efficiency is carried out.

As shown above, the optimization problem is formulated as the minimization problem for objective function (4) subject to the box constraints (5) and (6). In the following section, we show utilization of the optimization algorithm in the present research.

6 The present algorithm

One important technical point associated with solving the weather-routing optimization problem using the real-coded GA is how to treat infeasible points. There are two types of infeasibility in the weather-routing problem. The first type is infeasible points that do not satisfy the constraint inequalities $g_i(x) \leq 0$. The second type is infeasible points that are outside the domain of the objective functions. In the first type, infeasible points are repaired by putting them on the boundary of the constraints violated by the points. The problem is the second type. Out-of-domain infeasibility occurs when a numerical simulation of weather routing to evaluate the objective functions terminates abnormally. It is impossible to know whether a point is out of domain without a numerical simulation. Therefore, no repair operator is available.

We treat infeasibility in the following manner. (1) If a point violates the rectangular constraint, we put it on the nearest boundary of the rectangular constraint. (2) If the point to be repaired is outside of the domain of the objective function, we discard the point and sample and evaluate a new point.

The algorithms of JGG and REX$^{\text{star}}\left(\mathcal{U}, N_{\text{p}}\right)$ are described in Algorithms 1 and 2. The notation used in these tables is summarized as follows:

InitLowerBound:	n-dimensional vector whose ith element is the lower bound of the population initialization in the ith coordinate
InitUpperBound:	n-dimensional vector whose ith element is the upper bound of the population initialization in the ith coordinate
N_{pop}:	population size
N_{p}:	number of parental points
N_{c}:	number of offspring points
t:	step-size parameter for REX$^{\text{star}}$

The initialization region is basically the whole space satisfying the rectangular constraint. The number of parental points suggested is $n + 1$. The number of offspring points is set to $N_{\text{c}} = 4n$. Parameter tuning is required for the population size N_{pop} and step-size t for REX$^{\text{star}}\left(\mathcal{U}, N_{\text{p}}\right)$.

Algorithm 1 JGG

1: *Population initialization*. Sample initial population independently and uniform randomly in [InitLowerBoundi, InitUpperBoundi] for each coordinate. Evaluate the objective function values of the population. If some points are out of domain, then discard the infeasible points and repeat to sample new points and evaluate their objective function values until all points are feasible.

2: *Selection for reproduction*. Select N_{p} points randomly from the current population and denote them by $y_1, y_2, \ldots, y_{N_{\text{p}}}$.

3: *Crossover*. Produce and evaluate N_{c} offspring points $z_1, z_2, \ldots, z_{N_{\text{c}}}$ by REX$^{\text{star}}\left(\mathcal{U}, N_{\text{p}}\right)$.

4: *Selection for survival*. Replace $y_1, y_2, \ldots, y_{N_{\text{p}}}$ with the best N_{p} offspring points $z_{(1)}, z_{(2)}, \ldots, z_{(N_{\text{p}})}$ with respect to their objective function values. Then the next population becomes $\left\{x_1, x_2, \ldots, x_{N_{\text{pop}}}\right\} \setminus \left\{y_1, y_2, \ldots, y_{N_{\text{p}}}\right\} \cup \left\{z_{(1)}, z_{(2)}, \ldots, z_{(N_{\text{p}})}\right\}$.

5: Repeat steps 2–4 until a termination criterion is satisfied.

Algorithm 2 REX$^{\text{star}}\left(\mathcal{U}, N_{\text{p}}\right)$

1: Compute the mean of parental points $y_g = \frac{1}{N_{\text{p}}} \sum_{i=1}^{N_{\text{p}}} y_i$.

2: Generate mean-symmetric points for all parents: $\bar{y}_i = 2y_g - y_i$..

3: If some mean-symmetric points violate the rectangular constraint, put them on the nearest boundary of the constraint.

4: Evaluate the objective function values of mean-symmetric points.

5: Compute the mean of the best N_{p} points $v_1, v_2, \ldots, v_{N_{\text{p}}}$ among $\{y_i\} \cup \{\bar{y}_i\}$ with respect to their objective function values: $y_b = \frac{1}{N_{\text{p}}} \sum_{i=1}^{N_{\text{p}}} v_i$.

6: Discard infeasible mean-symmetric points and let K be the set of feasible mean-symmetric points.

7: **while** $|K| < N_{\text{c}}$ **do**

8: Generate a new candidate as

$$z = y_g + \text{diag}(\zeta_1, \zeta_2, \cdots, \zeta_n)\left(y_b - y_g\right) + \sum_{i=1}^{N_{\text{p}}} \xi_i \left(y_i - y_g\right),$$

where ζ_i and ξ_i are uniform random values in $[0, t]$ and $\left[-\sqrt{3/N_{\text{p}}}, \sqrt{3/N_{\text{p}}}\right]$, respectively.

9: If the candidate point violates the rectangular constraint, put it on the nearest boundary of the constraint.

10: Evaluate the objective function value. Add the point to K, $K = K \cup \{z\}$, if it is feasible, otherwise discard it.

11: **end while**

12: Return the set K of N_{c} feasible points.

7 Subject ship

In the present study, the subject ship for test calculation is the ITTC SHIP A-1 container ship, which was used for the ITTC benchmark testing study of intact stability in following and stern quartering waves [24]. The body plans and principal specifications are shown in Fig. 1 and Table 1, respectively. In Table 1, ASS denotes the lateral projected area of the superstructure. Despite the fact that its bow flare and transom stern are not very exaggerated, parametric rolling was observed in following and quartering seas [25] as well as head seas [26]. Moreover, even capsizing events were observed, particularly in following seas with a GM of 0.15 m [25].

In this research, 1.0 m is chosen as the metacentric height (GM), since parametric rolling was experimentally observed in head seas with this GM value. Further, given that this ship is intended for use in research into ship stability in the tank test, detailed information about the superstructure—which is necessary to estimate surge wind-induced force—is lacking. Therefore, the authors determined the size and location of the superstructure and the coefficients necessary to estimate this force, as shown in Table 1.

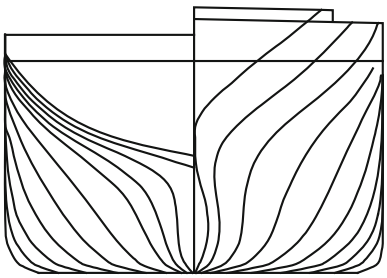

Fig. 1 Body plan of ITTC ship A-1

Table 1 Specifications of ITTC ship A-1

Item	Value
Length between perpendiculars: L_{pp}	150.0 m
Breadth: B	27.2 m
Depth: D	13.5 m
Mean draught: T	8.5 m
Block coefficient: C_b	0.667
Ship weight: W	23710 ton
Pitch radius of gyration: κ_{yy}/L_{pp}	0.244
Longitudinal position of center of gravity from the midship: x_{cg}	1.01 m aft
Metacentric height: GM	1.0 m
Natural roll period: T_ϕ	20.1 s
Propeller diameter: D_p	5.04 m
Thrust deduction coefficient: t_p	0.206
Effective propeller thrust: w_p	0.250
Bilge keel area: A_B	22.5 m^2
Breadth of bilge keel: L_B	0.549 m
Transverse projected area: A_T	585.7 m^2
Lateral projected area: A_L	2311 m^2
Lateral projected area of superstructure: A_{OD}	1332 m^2
Distance from midship section to center of lateral projected area: C	−5.095 m
Distance from midship section to center of the ASS: C_{BR}	−65.43 m
Height to top of superstructure: H_{BR}	22.34 m
Height to center of lateral projected area: H_C	7.550 m

8 Calculation results

To demonstrate the validity of the proposed method, a test calculation was carried out for the eastbound trans-Pacific voyage of ITTC ship A-1. On departing near Japan (35°40′N, 141°55′W) at 1200z on 22 December 2008, the ETA was set to 0500z 1 January 2009 near Seattle (48°33′N, 126°E). As stated in Sect. 5, to calculate f_1 we must calculate the energy E_A necessary for the voyage along the great-circle route with a constant propeller revolution number. Here, we set the propeller revolution to that number, which enables the ship to arrive at 0445z on 1 January 2009. Here, the waypoints are set in units of longitude of 5°. Table 2 shows the parameters employed in the optimization using RCGA. In the present research, the existence of islands is not fully considered; considering the lack of weather forecasting data for such islands, such a route is treated as an infeasible solution and it is discarded at the optimization stage. Therefore, the existence of a relatively small island is not taken into account.

For the purposes of comparative study, route optimization is carried out for all three objective functions: Obj1, Obj2 and Obj3. Iterative methods such as the GAs require that the control vector x is initialized at the beginning. Concerning the initial values of the latitudes of the waypoints, $\mathrm{Lat}_1, \ldots, \mathrm{Lat}_{\mathrm{INode}}$, two types of initializations (Int1 and Int2) are applied. In the case of Int1, the routes prepared for RCGA are initialized within the box-constrained

Table 2 Parameters used in RCGA

Item	Value
Number of waypoints: INode	18
Dimension of vector to be optimized: n	37
Population size: N_{pop}	$5n$
Step-size parameter for REX^{star}: t	4
Maximum number of generations	2000

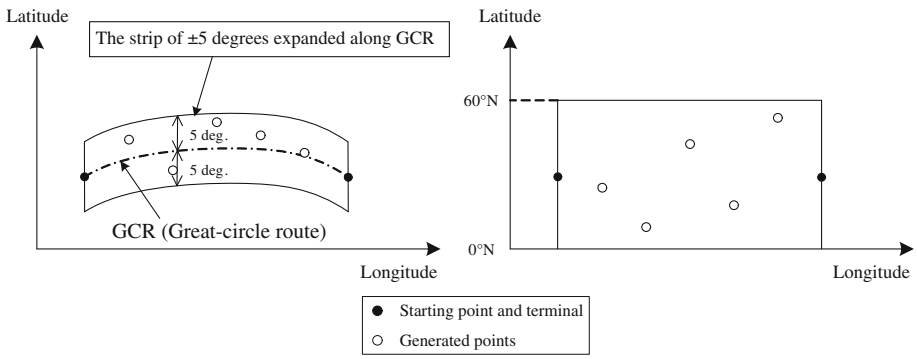

Fig. 2 Schematic view of the two initializations, Int1 and Int2. Here, the left figure indicates the Int2 initialization, whereas the right figure indicates the Int1 initialization

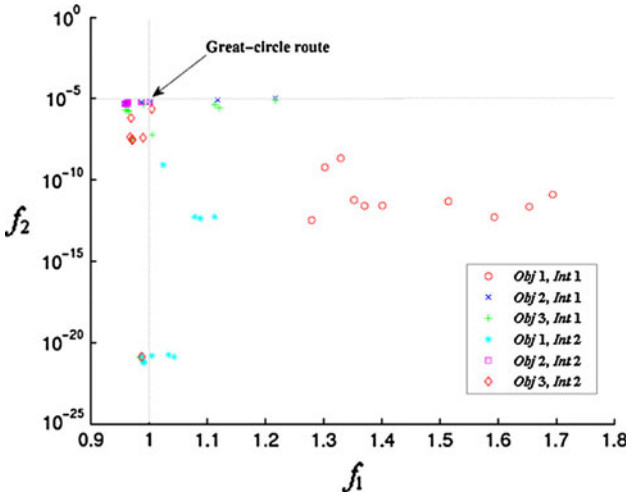

Fig. 3 Final calculation results with all combinations of objective functions and initializations

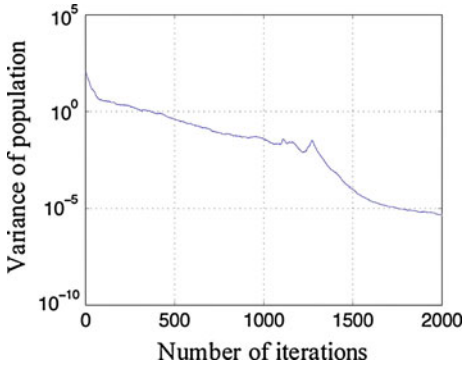

Fig. 4 The variance of the population in the case of Obj3

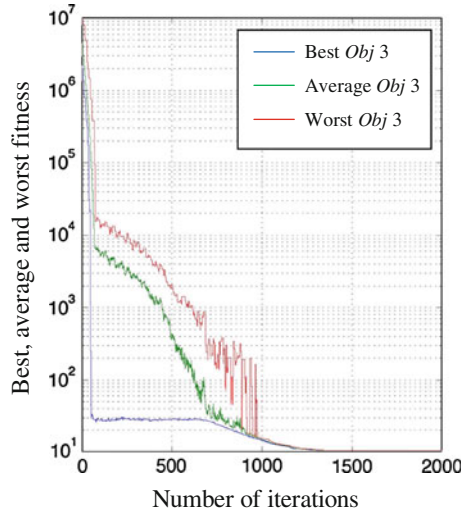

Fig. 5 The best, average and worst fitnesses for a typical trial in the case of Obj3

field, whereas, in the case of Int2, the initializations are done within the strip of ±5° expanded along the great-circle route in the latitude direction. Schematic views of these two initializations are shown in Fig. 2. In this figure, the initialization is carried out within the region enclosed by the solid line. Initialization of the propeller revolution number is carried out in the box constraint; i.e., Eq. 6. Route optimization is then conducted for all six combinations of objective functions and initializations, and ten trials with a different random seed for route initialization, Int1 and Int2, are conducted for each case. The results for the 60 cases are shown in Fig. 3. In this figure, the horizontal axis denotes the optimized function value of f_1, whereas the vertical axis denotes the value of f_2 on a logarithmic scale.

As can be observed in Fig. 3, the result depends on the random number of the initialization. Figure 4 indicates the variance of the population, whereas Fig. 5 shows the best, the average and worst fitnesses for a typical trial in the case of Obj3. As can be observed from this figure, the calculation using RCGA converges sufficiently for the trial. Therefore, the dispersion in the obtained solution observed in Fig. 3 implies the existence of many local solutions, so it can be assumed that the problem is a multimodal function problem. For such a problem, it is presumed that optimization cannot be conducted using the single-point search method. In contrast, GAs are robust for such problems, as mentioned above. Therefore, although the result depends

on a random number, a global search for a better solution can be successfully conducted.

From Fig. 3, it is clear that if the weight of the parametric rolling is increased, the fuel efficiency deteriorates. This fact implies that there is a trade-off between fuel efficiency and ship safety with respect to parametric rolling. Furthermore, the results obtained are distributed in the direction of the f_1 axis for every objective function. Although this trend is observed in more or less every case, it is especially noticeable in the trials with Int1 initialization of the waypoints. This result implies that the efficiency of route optimization can be improved by using Int2 initialization for all three objective functions. Therefore, to obtain the best solution, Int2 initialization is highly recommended.

As can also be seen in Fig. 3, the routes that have an f_1 value of <1.0 are successfully obtained with Obj2 and Int2, except for one trial. For practical purposes, however, since only the fuel efficiency is taken into account in the route optimization, we have to generate the route while realizing an f_1 value of <1.0. Therefore, when the ship route is optimized with Obj2 and Int2, it is highly recommended that optimizations with at least two or more random seeds in parallel are carried out, and then the best solution in these trials should be taken. Furthermore, when the risk of parametric rolling is taken into account, a larger number of trials with different seeds is recommended. Although, in the present research, the calculations are carried out for only three kinds of objective functions for comparative purposes, the appropriate weight should be determined through the optimization of several objective functions with different ratios between the fuel efficiency and ship safety in practice.

Table 3 shows the best results (that have the smallest value of f_1) among ten trials with different random seeds using each combination of the three objective functions and two initializations. Here, the f_1 and f_2 values calculated for the great-circle voyage with a constant propeller revolution number are listed in the first line. From this table, we can see the trade-off between fuel efficiency and safety in parametric rolling, as pointed out above.

In Figs. 6, 7, 8, 9, 10 and 11, the optimized routes for the six cases are shown as a solid line, and the great-circle route is shown as a dotted line. Note that, in Figs. 6 and 7, the ship takes a more northerly course in the sea near Japan in comparison with the other results. These two results are obtained for the case in which fuel efficiency is not significantly considered in the route optimization. Therefore, it is clear that these routes decrease the probability of parametric rolling for the weather conditions utilized in this paper.

Further, as an example, the data for the voyage corresponding to the case shown in Fig. 9 (Obj2, Int2) are

Table 3 Optimization results for each calculation condition

Objective function	Initialization	f_1	f_2
Initial condition	Initial condition	1.0	9.841×10^{-6}
Obj1	Int1	1.280	3.367×10^{-13}
Obj3	Int1	0.9594	2.071×10^{-6}
Obj2	Int1	0.9571	4.743×10^{-6}
Obj1	Int2	0.9869	1.441×10^{-21}
Obj3	Int2	0.9673	4.312×10^{-8}
Obj2	Int2	0.9586	4.729×10^{-6}

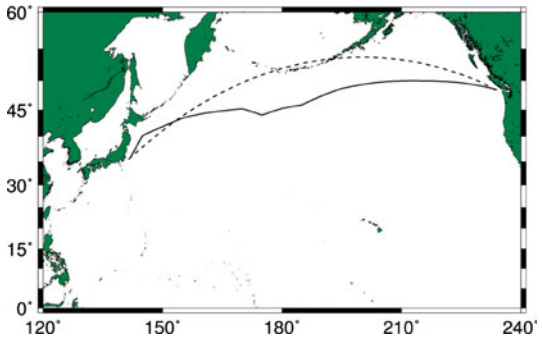

Fig. 6 Optimum route for the combination of Obj1 and Int1

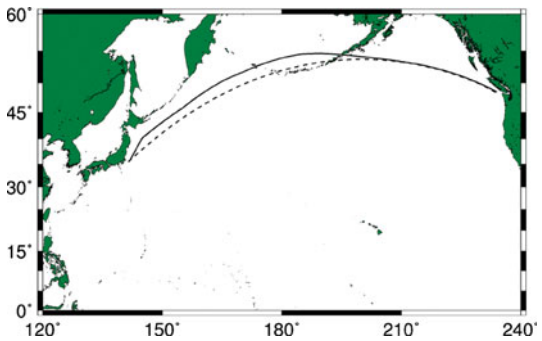

Fig. 7 Optimum route for the combination of Obj1 and Int2

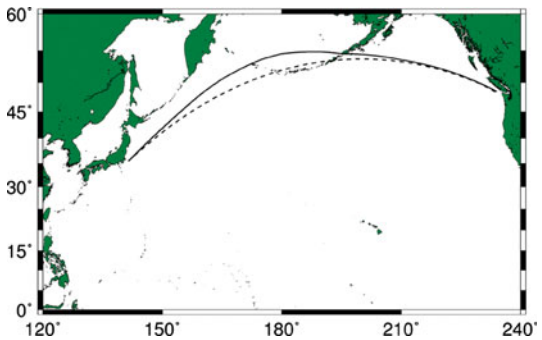

Fig. 8 Optimum route for the combination of Obj2 and Int1

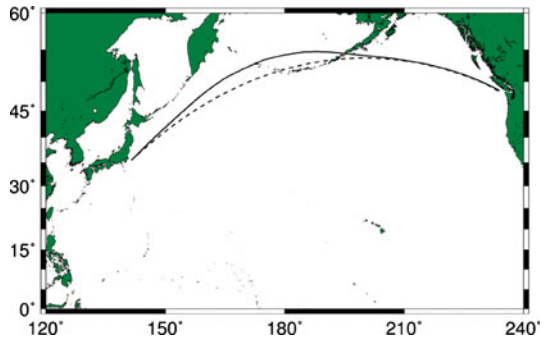

Fig. 9 Optimum route for the combination of Obj2 and Int2

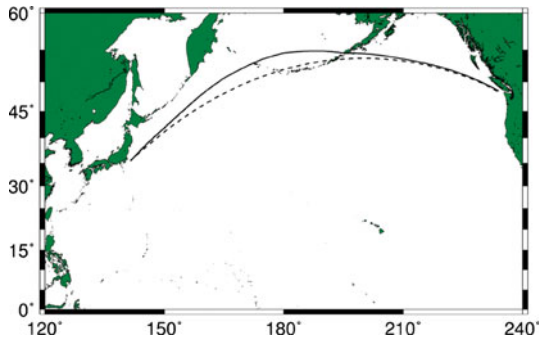

Fig. 10 Optimum route for the combination of Obj3 and Int1

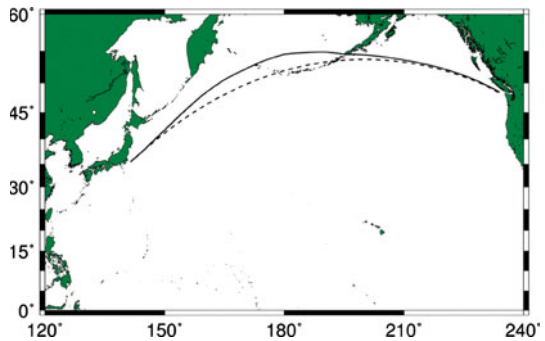

Fig. 11 Optimum route for the combination of Obj3 and Int2

shown as a function of the ship position in Figs. 12, 13, 14, 15, 16, 17, 18 and 19. These figures show the propeller revolution number, ship's forward velocity, ship's course, wave direction measured from the fixed coordinate system, significant wave height, mean wave period, added resistance, and parametric rolling probability, respectively. In these figures, a solid line indicates the optimum result and a dotted line denotes the result corresponding to the voyage along the great-circle route with a constant propeller revolution number. From these figures, we notice that the optimized route occurs across the sea with a lower

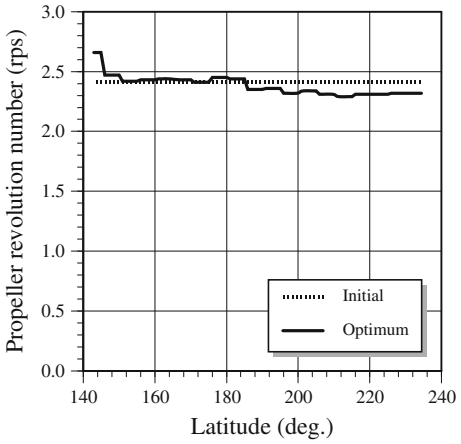

Fig. 12 Comparison of the propeller revolution number between the initial route and the optimized route

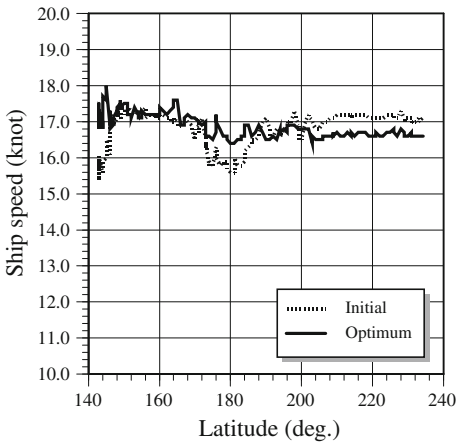

Fig. 13 Comparison of the ship's speed between the initial route and the optimized route

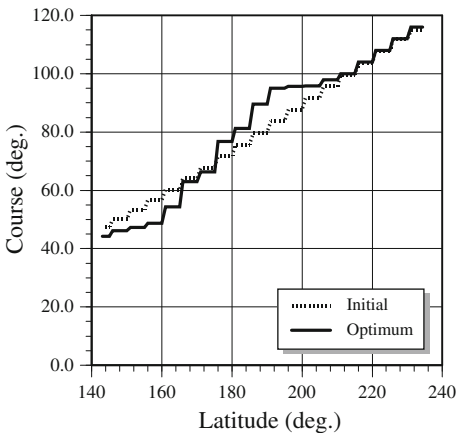

Fig. 14 Comparison of the ship's course between the initial route and the optimized route

significant wave height than the great-circle voyage. As a result, this optimized route successfully reduced the added resistance around 180°W, so that the distribution of the

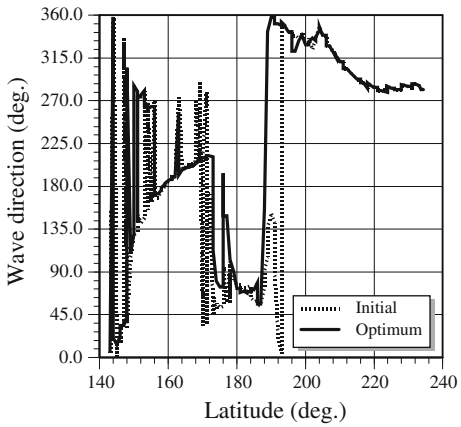

Fig. 15 Comparison of the wave direction between the initial route and the optimized route

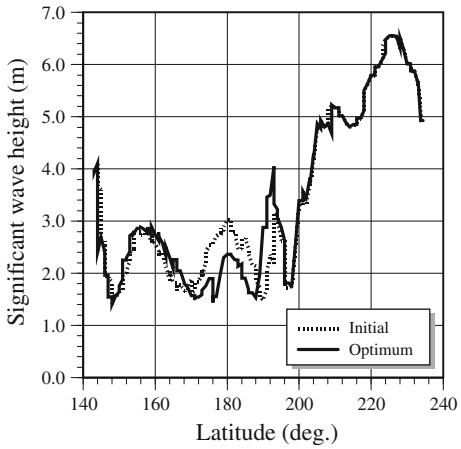

Fig. 16 Comparison of the significant wave height between the initial route and the optimized route

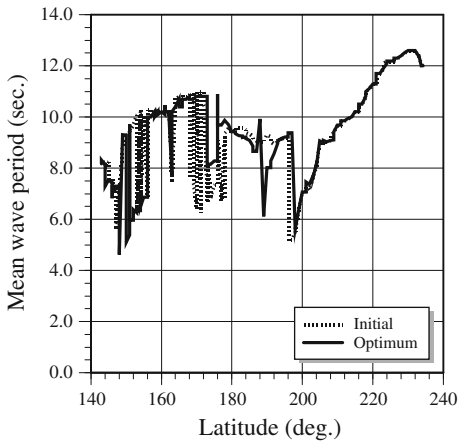

Fig. 17 Comparison of the mean wave period between the initial route and the optimized route

ship speed decreased. It can be observed that the parametric rolling probability shows a relatively large value in the sea near Japan. From this trend, we notice that the ship

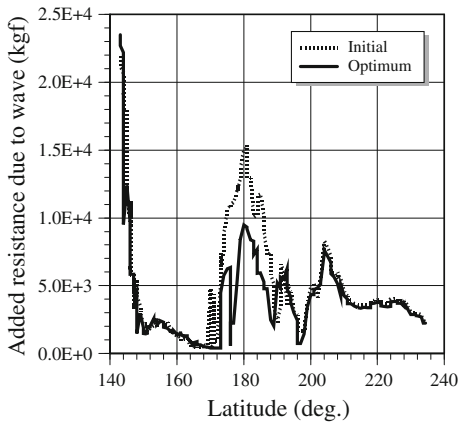

Fig. 18 Comparison of the added resistance between the initial route and the optimized route

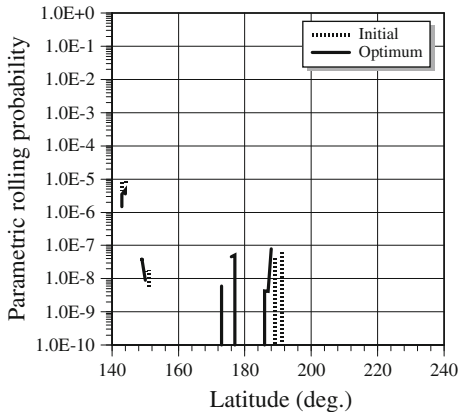

Fig. 19 Comparison of the parametric rolling probability between the initial route and the optimized route

routes shown in Figs. 6 and 7 avoid the rough sea due to the large parametric rolling probability. Further, from Fig. 18, we can see that in head seas, the added resistance and the parametric rolling probability simultaneously show large values with a large significant wave height for both routes. This result implies that there is at least some correlation between the added resistance and the parametric rolling probability, and it is most likely that the two values become large in severe head seas. Therefore, this consideration implies that some of the parametric rolling probability can be reduced even if only the fuel efficiency is considered in the objective function. In actuality, although Obj2 is utilized as the objective function in this example, the risk of parametric rolling is slightly reduced.

Finally, we show comparisons of the significant wave height and the parametric rolling probability between the optimized routes for (Obj1, Int1) and (Obj2, Int2) in Figs. 20 and 21, respectively. From Fig. 20, note that in the region in which the parametric rolling probability is high,

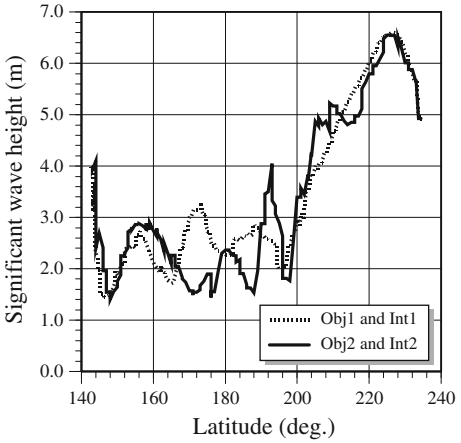

Fig. 20 Comparison of the significant wave heights of the optimized routes for (Obj1, Int1) and (Obj2, Int2)

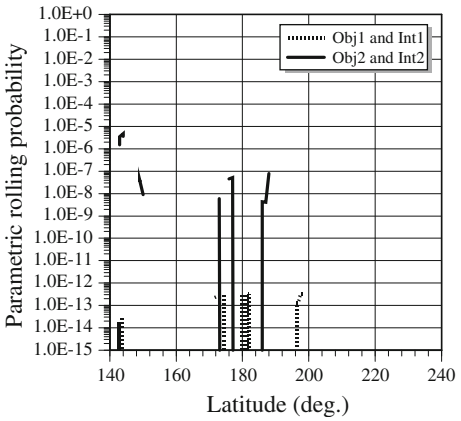

Fig. 21 Comparison of the parametric rolling probabilities of the optimized routes for (Obj1, Int1) and (Obj2, Int2)

namely in the sea near Japan, there is a relatively small difference in the significant wave heights of the two routes. Therefore, in this region, changing the ship's direction relative to the wave direction—thus avoiding the dangerous head sea conditions—leads to a drop in the probability. It should also be noted that by using the proposed method, meaningful and useful solutions are successfully generated for each objective function.

In these optimizations, one trial can be carried out within a few hours on a typical PC, so the proposed optimization method does not have a large computational cost—it is small enough to be practical. As stated at the beginning of this section, in the present research, the existence of islands is not fully considered. For practical purposes, it would be accounted for using topographical map data. If an island exists along the ship's route generated during the optimization process, this solution is infeasible and must be discarded. Thus, we can conclude that the present route optimization method using RCGA is also quite robust to geographical infeasibility.

9 Concluding remarks

This paper proposes a route optimization method based on the use of RCGA. The principal conclusions drawn from this work can be summarized as follows:

1. Route optimization for an oceangoing vessel can be robustly and stably conducted using the proposed method. In addition, initialization of the routes for RCGA should be carried out along the great-circle route in order to robustly search for the optimum solution.
2. The risk of parametric rolling is taken into account in the route optimization, and we have confirmed that it is easy to obtain a route that reduces the parametric rolling probability using the proposed method.
3. For the conditions employed for the calculation described in this paper, the risk of parametric rolling is slightly decreased even if that risk is not taken into account in the objective function.
4. Considering its robustness when searching for the optimum route, this method appears to be a powerful practical tool by choosing the appropriate weights to apply to the fuel economics and the ship's safety to parametric rolling.

In the present method, the risk of parametric rolling is simply taken into account as its probability for unit time. However, the maximum roll angle or the length of time in which the ship is exposed in the sea can trigger this phenomenon, and these are not taken into account in this work. We will consider these conditions in future work. Furthermore, in the present research, the model of the engine system has been simplified. In the future, this model will be improved for practical purposes.

Acknowledgments The short-term prediction of the added resistance and acceleration of the bow section was obtained by using the RIOS (Research Initiative on Oceangoing Ships) system developed at Osaka University. The authors are grateful to members of the RIOS for their support.

Appendix: The translation of allowable failure probability from its value per year to its value per second

Let the occurrence probability per second of a random event be p_{second}. Its probability per year p_{annual} can be calculated using the relation for the complementary event:

$$p_{\text{annual}} = 1 - (1 - p_{\text{second}})^{3600 \cdot 24 \cdot 365}. \quad \text{(A1)}$$

If we expand the above equation using the binominal theorem and assume that p_{second} is sufficiently small, then the following equation is obtained:

$$p_{\text{annual}} \approx 3600 \cdot 24 \cdot 365 \cdot p_{\text{second}}. \quad \text{(A2)}$$

Here, substitution of the threshold value 10^{-6} into p_{annual} yields the final result, as follows:

$$p_{\text{second}} \approx 3.17 \times 10^{-14}. \quad \text{(A3)}$$

References

1. Takashima K, Hagiwara H, Shoji R (2004) Fuel saving by weather routing—simulation using actual voyage data of the container ship. J Jpn Inst Navig 111:259–266 (in Japanese)
2. Tsujimoto M, Tanizawa K (2005) Development of a weather adaptive navigation system: influence of weather forecast. J Jpn Soc Navl Archit Ocean Eng 2:75–83 (in Japanese)
3. Hashimoto H, Umeda N, Ogawa Y, Taguchi H, Iseki T, Bulian G, Toki N, Ishida S, Matsuda A (2008) Prediction methods for parametric rolling with forward velocity and their validation—Final Report of the SCAPE Committee (Part 2). In: Proc 6th Osaka Colloquium on Seakeeping and Stability of Ships, Osaka, Japan, 26–28 March 2008, pp 265–275
4. France WN, Levadou M, Treakle TW, Paulling JR, Michel RK, Moore C (2003) An investigation of head-sea parametric rolling and its influence on container lashing systems. Mar Technol 40:1–19
5. Eshelman LJ (1993) Real-coded genetic algorithms and interval-schemata. In: Whitley LD (ed) Proceedings of the Second Workshop on Foundations of Genetic Algorithms, Vail, Colorado, USA, July 26–29 1992. Morgan Kaufmann, Burlington, pp 187–202
6. Ono I, Kobayashi S (1997) A real-coded genetic algorithm for function optimization using unimodal normal distribution crossover. In: Proc 7th Int Conf on Genetic Algorithms, East Lansing, MI, USA, 19–23 July 1997, pp 246–253
7. Maruo H (1960) Wave resistance of a ship in regular head seas. Bull Fac Eng Yokohama Natl Univ 9:73–91
8. Kashiwagi M (1995) Prediction of surge and its effect on added resistance by means of the enhanced unified theory. Trans West-Japan Soc Nav Arch 89:77–89
9. Kashiwagi M (1997) Numerical seakeeping calculations based on the slender ship theory. Schiffstechnik 4(4):167–192
10. Fujiwara T, Ueno M, Nimura T (1998) Estimation of wind forces and moments acting on ships. J Soc Nav Archit Jpn 183:77–90 (in Japanese)
11. Maki A, Umeda N, Shiotani S, Kobayashi E (2011) Parametric rolling prediction in irregular seas using combination of deterministic ship dynamics and probabilistic wave theory. J Mar Sci Technol (accepted)
12. Blocki W (1980) Ship safety in connection with parametric resonance of the roll. Int Shipbuild Prog 27(306):36–53
13. Longuet-Higgins MS (1984) Statistical properties of wave groups in a random sea state. Proc R Soc Lond Ser A 312:219–250
14. Kita H, Ono I, Kobayashi S (1998) Theoretical analysis of the unimodal normal distribution crossover for real-coded genetic algorithms. In: Proc IEEE Congr on Evolutionary Computation, Anchorage, AK, USA, 4–9 May 1998, pp 529–534
15. Kita H, Yamamura M (1999) A functional specialization hypothesis for designing genetic algorithms. In: Proc 1999 IEEE Int Conf on Systems, Man, and Cybernetics, Tokyo, Japan, 12–15 Oct 1999, pp 579–584
16. Kita H, Ono I, Kobayashi S (1999) Multi-parental extension of the unimodal normal distribution crossover for real-coded genetic algorithms. In: Proc IEEE Congr on Evolutionary Computation, Washington, DC, USA, 6–9 July 1999, pp 1581–1588
17. Tsutsui S, Yamamura M, Higuchi T (1999) Multi-parent recombination with simplex crossover in real coded genetic algorithms. In: Proc Genetic and Evolutionary Computation Conf, GECCO, Orlando, FL, USA, 13–17 July 1999, pp 657–664
18. Sakuma J, Kobayashi S (2005) Latent variable crossover for k-tablet structures and its application to lens design problems. In: Proc Genetic and Evolutionary Computation Conf, GECCO, Washington, DC, USA, 25–26 June 2005, pp 1347–1353
19. Kobayashi S (2009) The frontiers of real-coded genetic algorithms. Trans Jpn Soc Artif Intell 24(1):147–162 (in Japanese)
20. Akimoto Y, Nagata Y, Sakuma J, Ono I, Kobayashi S (2010) Analysis of the behavior of MGG and JGG as a selection model for real-coded genetic algorithms. Trans Jpn Soc Artif Intell 25(2):281–289 (in Japanese)
21. Akimoto Y, Sakuma J, Ono I, Kobayashi S (2009) Adaptation of expansion rate for real-coded crossovers. In: Proc 11th Annual Conf on Genetic and Evolutionary Computation, GECCO '09, Montréal, Canada, 8–12 July 2009, pp 739–746
22. Satoh H, Yamamura M, Kobayashi S (1996) Minimal generation gap model for GAs considering both exploration and exploitation. In: Proceedings of IIZUKA '96, Iizuka, Japan, 30 Sept–5 Oct 1996, pp 494–497
23. Konishi I, Takaoka N, Ishikawa H (1984) Structural safety and reliability. Maruzen, Tokyo [in Japanese; original: Schueller GI (1981) Einfuhrung in die Sicherheit und Zuverlassigkeit von Tragwerken. Wilhelm Ernst & Sohn, Munich]
24. Umeda N, Renilson MR (2001) Benchmark testing of numerical prediction on capsizing of intact ships in following and quartering seas. In: Proc 5th Int Workshop on Stability and Operational Safety of Ships, Trieste, Italy, 12–13 Sept 2001, pp 6.1.1–6.1.10
25. Umeda N, Hamamoto M, Takaishi Y, Chiba Y, Matsuda A, Sera W, Suzuki S, Spyrou KJ, Watanabe K (1995) Model experiments of ship capsize in astern seas. J Soc Nav Archit Jpn 177:207–217
26. Umeda N, Hashimoto H, Minegaki S, Matsuda A (2008) An investigation of different methods for the prevention of parametric rolling. J Mar Sci Technol 13(1):16–23